Catecholic Chemistry To Obtain Recyclable and Reusable Hybrid Polymeric Particles as Catalytic Systems

ARTICLE *in* MACROMOLECULES · APRIL 2013

Impact Factor: 5.8 · DOI: 10.1021/ma4003566

4 AUTHORS, INCLUDING:

Gema Marcelo
University of Alcalá
30 PUBLICATIONS **298** CITATIONS
SEE PROFILE

Marta Fernández-García
Spanish National Research Council
160 PUBLICATIONS **2,096** CITATIONS
SEE PROFILE

Macromolecules

Article

pubs.acs.org/Macromolecules

Catecholic Chemistry To Obtain Recyclable and Reusable Hybrid Polymeric Particles as Catalytic Systems

Marta Álvarez-Paino, Gema Marcelo, Alexandra Muñoz-Bonilla,* and Marta Fernández-García*

Instituto de Ciencia y Tecnología de Polímeros (ICTP-CSIC), C/Juan de la Cierva 3, 28006-Madrid, Spain

ABSTRACT: A straightforward approach was proposed to decorate gold nanoparticles onto recyclable supports based on magnetite/polymer composite materials for highly efficient catalysis. Cross-linked particles bearing a controllable content of catechol active residues were synthesized by precipitation polymerization of mussel-inspired monomer, dopamine methacrylamide, and ethylene glycol dimethacrylate. The magnetite nanoparticles were also surface modified with dopamine derivatives to introduce vinyl or catechol groups. Then, the magnetite nanoparticles with vinyl groups were incorporated inside of the polymeric particles forming a magnetic core during the precipitation polymerization. As an alternative pathway to achieve these efficient catalytic systems, magnetic nanoparticles functionalized with dopamine were immobilized at the surface of the polymeric particles via Michael addition. Then, catechol redox chemistry was used to form and anchor gold nanoparticles on the surface of both synthesized magnetic supports. Subsequently, we investigated the catalytic activity and reusability of the magnetic composite catalysts toward the reduction of 4-nitrophenol to 4-aminophenol by sodium borohydride. The systems with high gold content undergo great catalytic performance. Besides, the prepared catalysts can be easily recovered from the reaction mixture and reused several times.

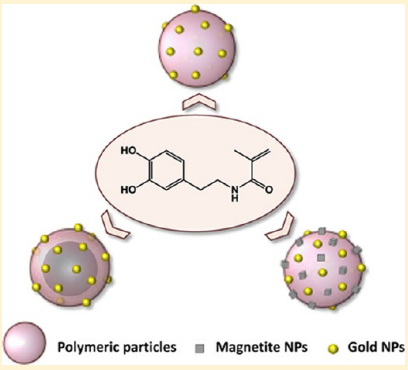

INTRODUCTION

Nowadays, the chemistry of catechol containing molecules has gained a great interest as a surface modification agent in a wide range of applications,[1−3] as a consequence of their ability to strongly adhere to any organic or inorganic surfaces including metals, metal oxides, alumina, silica, mica, ceramics and polymers.[4] Although the adhesion mechanism is not fully understood, in all the proposed mechanisms, the catechol groups form strong interactions such as hydrogen-bonding, p-electron or bidentate bonding through the hydroxyl groups. Besides, under oxidizing conditions, the catechol groups can be oxidized to generate *o*-quinone functionality, which is highly reactive with various functional groups including thiol, amine, and quinone itself via Michael-type additions or Schiff base reactions. On the basis of this reaction, the oxidized quinone of dopamine can react to form a cross-linked polymer matrix via spontaneous oxidative polymerization. Moreover, catechol derivatives have demonstrated to be good reducing agents, which can be employed to synthesize metal NPs directly from the reduction of metal salts.[5,6] All these characteristics, for instance, outstanding adhesion, self-polymerization and reduction, provide a huge variety of possibilities to fabricate new materials following facile and mild procedures and, at the same time, environmental friendly reactions conditions. This versatile catecholic chemistry has been extensively used to create hybrid materials in practical applications, mostly biological but also others such as catalytic[7] or in solar cell applications.[8] In this framework, iron oxide nanoparticles have been modified through catecholic chemistry in order to increase colloidal stability or to incorporate desired functionalities.[9−11] Magnetite nanoparticles (Fe_3O_4 NPs) are particularly attractive due to their superparamagnetic properties, nontoxicity and biocompatibility.[12] Thus, Fe_3O_4 NPs have been investigated in various biomedical applications, for example, as contrast agents in magnetic resonance imaging (MRI),[13] hyperthermia therapy,[14,15] biological separation,[16] or drug delivery.[17] Moreover, the recovery and reuse of catalysts have become nowadays important factors from the ecological and economical points of view. Therefore, they have been incorporated in catalytic systems for numerous organic reactions, taking advantage of the efficient and facile separation of magnetic particles from suspensions.[18−22]

In this article we prepare different polymeric and hybrid particles as a recyclable supports of gold nanoparticles for highly efficient catalytic systems (see Scheme 1). For this purpose we use facile and straightforward strategies making use of the catecholic chemistry in several paths. The protocol is basically based on the preparation of cross-linked particles bearing dopamine residues via precipitation polymerization of dopamine methacrylamide and ethylene glycol dimethacrylate. The magnetite nanoparticles are incorporated inside of the particles forming a magnetic core or at the surface of the particles. In both cases the particles are immobilized thought the catechol groups. Then, the gold nanoparticles are formed and anchored on the surface of the particles directly in an aqueous solution of hydrogen tetrachloroaurate without the addition of any exogenous reducing agent due to the capability of the catechols to reduce metal cations into neutral metal

Received: February 19, 2013
Revised: March 27, 2013
Published: April 4, 2013

   dx.doi.org/10.1021/ma4003566 | *Macromolecules* 2013, 46, 2951−2962

Scheme 1. (A) Chemicals Structures of the Starting Products Used and (B, C and D) Synthetics Approaches Followed to Obtain the Different Hybrid Polymeric Systems Designed

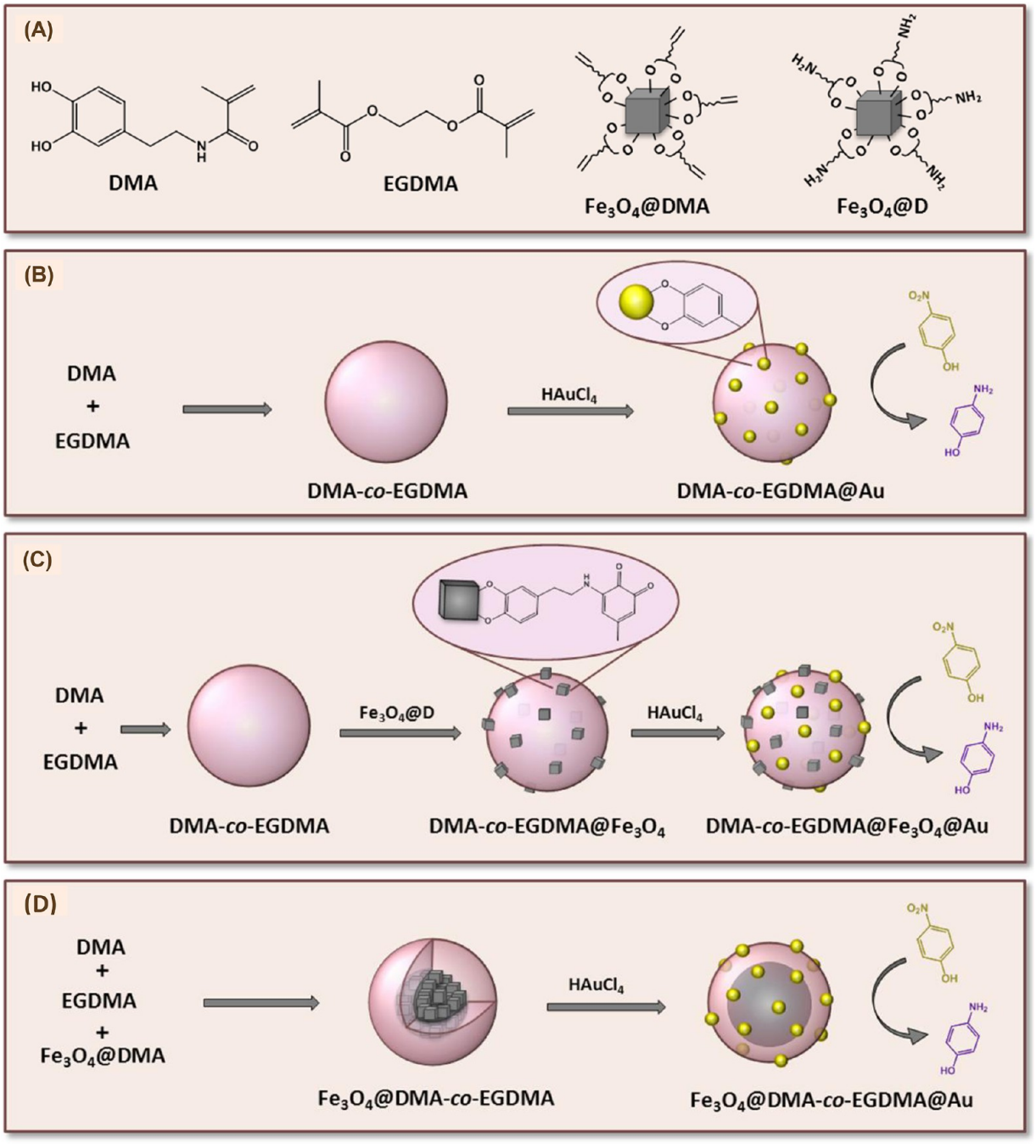

atoms. Gold nanoparticles (Au NPs), in particular, are of great interest because their catalytic activity in a number of chemical reactions in most cases under soft condition and even at ambient temperature.[23] It is well-known that the catalytic activity of gold is directly related to the particle size, requiring sizes in the nanometer length scale.[24−26] Therefore, the separation of the very small particle from the medium entails difficulties that are normally solved by dispersing the Au NPs on support materials in order to enhance the stability and to facilitate the catalyst recovery.[27] To this respect, the magnetically recoverable supports for the immobilization of Au NPs present important advantages compared to others materials such as oxides, polymers, carbon-based solids, or hybrids.[28,29] In fact, magnetic separation at the end of each catalytic cycle is considered easy, fast, and very efficient, constituting, at the same time, more sustainable and environmentally friendly process since it diminishes the catalyst mass losses and avoids the use of additional solvents or other substances.

EXPERIMENTAL SECTION

Materials. Iron(III) acetylacetonate, oleic acid, dibenzyl ether, sodium hydroxide (NaOH), chlorhydric acid (HCl), triethylamine (TEA) were all purchased from Aldrich and used as received. 2,2′-Azobis(isobutyronitrile) (AIBN, Fluka) was purified by successive recrystallizations from methanol. The ethylene glycol dimethacrylate (EGDMA) was supplied by

dx.doi.org/10.1021/ma4003566 | Macromolecules 2013, 46, 2951−2962

Aldrich. The dopamine methacrylamide (DMA) was prepared and characterized according to a modified method[30] based on a previously reported strategy.[31] Hydrogen tetrachloroaurate(III) ($HAuCl_4$) and sodium borohydride ($NaBH_4$) were obtained from Alfa Aesar and Aldrich, respectively. The analytical reagents grade solvents acetonitrile (ACN), dimethylformamide (DMF), acetone, methanol, ethanol, and tetrahydrofuran (THF) as well as 4-nitrophenol (4-NP), were obtained from Scharlau.

Synthesis of Gold-Decorated Polymeric Particles (Scheme 1B). *Synthesis of the Polymeric Microparticles Containing Dopamine Groups (DMA-co-EGDMA).* The synthesis of particles was carried out by precipitation polymerization of dopamine methacrylamide and ethylene glycol dimethacrylate. The proportion of comonomers was varied in order to obtain particles with diverse content of active catechol groups and different cross-linking density, i.e., DMA/EGDMA: 80/20, 55/45, and 20/80 wt %. The total amount of monomers respects to the solvent was set at 1.8 wt %, and 4.5 wt % of AIBN initiator with respect to the total amount of the monomers was used. All the polymerizations were carried out in 10 mL vials closed under argon atmosphere. Vials were held perpendicular by a rotor and agitated with external (mechanical) and magnetic agitation. The agitation rate was fixed at 300 and 560 rpm for mechanical and magnetic stirrer, respectively. In a typical polymerization (DMA/EGDMA: 55/45), 0.1 g (0.45 mmol) of DMA and 0.084 g (0.42 mmol) of EGDMA were placed into the vial and dissolved in 10 mL of ACN. Subsequently, 8.2 mg of AIBN was added to the solution and the system was then heated up to 85 °C to initiate the polymerization. The reaction was allowed to proceed during 24 h. Afterward, the particles were recovered after centrifugation and then washed with ACN and acetone repeatedly.

Decoration of the DMA-co-EGDMA Microspheres with Gold Nanoparticles (DMA-co-EGDMA@Au). In brief, 10 mg of DMA-*co*-EGDMA microspheres (55/45 wt %) were dispersed in 2 mL of ethanol by sonication. Subsequently, an aqueous solution of HAuCl4 (0.6 mM, 20 mL) was added into the polymeric particles dispersion and, then, the dispersion turns pink as a consequence of the growth and the stabilization of gold nanoparticles. The reaction was allowed to proceed during 5 h with vigorous shaking. The product, DMA-*co*-EGDMA@Au, was washed with ethanol several times and recovered after centrifugation.

Synthesis of Magnetite-Encapsulated and Gold Nanoparticles-Decorated Microparticles (Scheme 1C). *Synthesis of Magnetite Nanoparticles (Fe_3O_4 NPs).* Oleic acid-functionalized magnetite nanoparticles were synthesized according to previous report with slightly modifications.[32] Briefly, iron(III) acetylacetonate (1.10 g) was added to a mixture of oleic acid (1.13 g) and benzyl ether (51.30 g). The mixture was deoxygenated at room temperature for 1 h and then was heated to 200 °C for 2 h under argon atmosphere. The solution was heated to reflux at 298 °C during 1 h. After cooling to ambient temperature, a mixture of toluene and hexane was added to the solution. The solution was centrifuged in order to precipitate the Fe_3O_4 nanoparticles. The separated precipitate was washed several times with chloroform.

Functionalization of Magnetite Nanoparticles with DMA (Fe_3O_4@DMA NPs) and Dopamine (Fe_3O_4@D NPs). A bioinspired surface modification was used to introduce vinyl groups on magnetite nanoparticles.[33,34] The oleic acid coating of the previously obtained magnetite nanoparticles was exchanged with DMA. The oleic acid-stabilized Fe_3O_4 NPs (15 mg) were dispersed in 3 mL of DMF and 250 mg of DMA was added to the mixture. The dispersion was treated with a sonifier for 1 h (settings: 20% amplitude, 3 s turn on, and 2 s off). The particles were isolated with an external magnet and were rinsed with ethanol at least three times. Similar procedure was used for the functionalization of magnetite with dopamine (Fe_3O_4@D NPs).

Preparation of Magnetic DMA-co-EGDMA Particles (Fe_3O_4@DMA-co-EGDMA). The hybrid particles were prepared via seeded precipitation polymerization. In a typical synthesis, 270 mg (1.36 mmol) of EGDMA and 330 mg (1.49 mmol) of DMA were placed into the reactor and dissolved in 10 mL of ACN. Then, 20 mg of DMA modified magnetite nanoparticles dispersed in 20 mL of ACN was injected into the solution under mechanical stirring (600 rpm). The mixture was heated up to 85 °C and then 28 mg of AIBN was added to start the polymerization. The reaction was allowed to proceed during 4 h. Afterward, the particles were recovered with an external magnetic field and, subsequently, washed several times with ACN and acetone.

Decoration of Fe_3O_4@DMA-co-EGDMA with Gold Nanoparticles (Fe_3O_4@DMA-co-EGDMA@Au). The loading of gold nanoparticles onto the magnetic/polymeric particles was carried out as follows: 6 mg of Fe_3O_4@DMA-*co*-EGDMA particles was dispersed in 1 mL of ethanol by sonication. Then, an aqueous solution of $HAuCl_4$ (0.6 mM, 13 mL) was added into the particles dispersion and, immediately, deep purple appeared as a result of the gold nanoparticles formation. The reaction was allowed to proceed during 5 h with vigorous shaking. The final product, Fe_3O_4@DMA-*co*-EGDMA@Au, was recovered with an external magnetic field and purified by repeated washings with water and ethanol.

Synthesis of Polymeric Particles Decorated with Gold and Magnetite NPs (Scheme 1D). *Surface Decoration of the DMA-co-EGDMA Microspheres with Magnetite Nanoparticles (DMA-co-EGDMA@Fe_3O_4).* Dopamine-modified magnetite nanoparticles (Fe_3O_4@D NPs) were attached onto the surface of the polymeric DMA-*co*-EGDMA microspheres. The details were as follows: 10.5 mg of the DMA-*co*-EGDMA particles (55/45 wt %) and 0.8 mg of dopamine surface-modified magnetite nanoparticles were dispersed in 30 mL of DMF by sonication during 10 min. Subsequently, the reaction mixture was magnetically stirred for 90 min. Then, the obtained polymeric particles with magnetite NPs attached on their surface (DMA-*co*-EGDMA@Fe_3O_4) were separated from the solution using an external magnet and washed several times with DMF and ethanol.

Anchoring Gold Nanoparticles onto the Surface of DMA-co-EGDMA@Fe_3O_4 Particles (DMA-co-EGDMA@Fe_3O_4@Au). In a typical preparation of DMA-*co*-EGDMA@Fe_3O_4@Au hybrids, 10 mg of DMA-*co*-EGDMA@Fe_3O_4 particles was dispersed in 1 mL of ethanol. Successively, an aqueous solution of $HAuCl_4$ (0.6 mM, 20 mL) was added into the particles dispersion. The reaction was left under stirring during 5 h at room temperature, followed by a separating and rinsing process with methanol at least three times. At last, the resultant hybrid particles were dried.

Catalytic Reduction of 4-Nitrophenol to 4-Aminophenol in an Aqueous Medium. Catalytic properties of the synthesized particles decorated with gold nanoparticles were investigated via the reduction of 4-nitrophenol (4-NP) to 4-aminophenol (4-AP) with $NaBH_4$ as reducing agent under

dx.doi.org/10.1021/ma4003566 | Macromolecules 2013, 46, 2951−2962

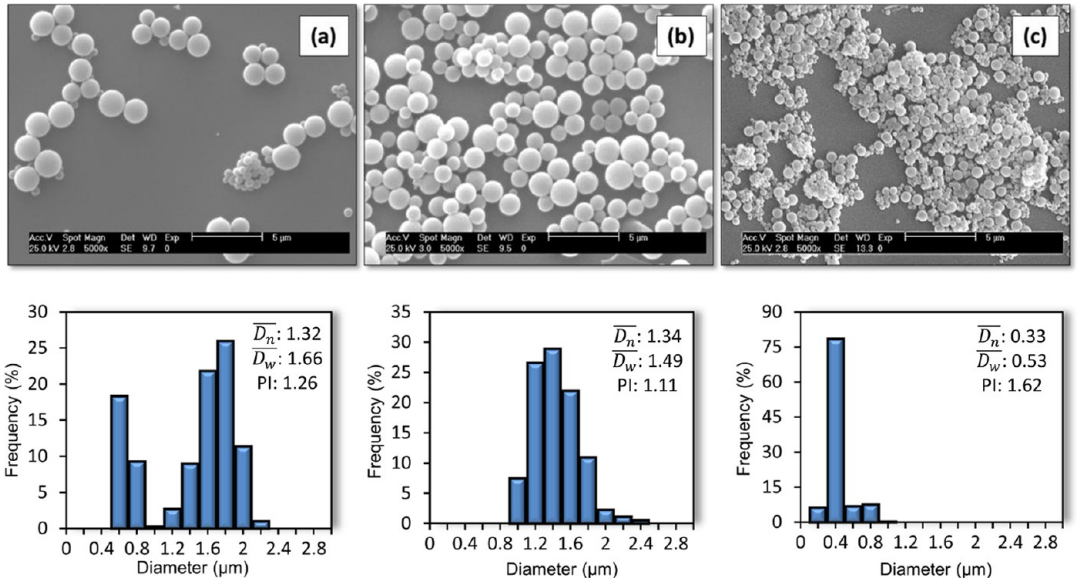

Figure 1. SEM images (top) and particle size distributions (bottom) of the synthesized DMA-*co*-EGDMA microspheres prepared by the precipitation polymerization with 4.5 wt % AIBN in acetonitrile at 85 °C. DMA/EGDMA ratio: (a) 80/20, (b) 55/45, and (c) 20/80 wt %.

ambient temperature in aqueous solution. In a typical experiment, 2 mL of 4-NP aqueous solution (0.1 mM) and 1 mL of $NaBH_4$ (0.2 M) aqueous solution were mixed in a quartz cuvette. Successively, the particles containing the gold nanoparticles (0.05 mg) were introduced into the mixture with gentle shaking. Visually, the yellow solution discolors gradually as the catalytic reaction proceeds. The catalytic activity was studied by UV−vis spectroscopy with a decrease at 400 nm in UV−vis absorption and a simultaneous increase in absorption at 300 nm, indicating the formation of 4-AP.

Measurements. The Fourier transform infrared (FTIR) spectra of KBr pellets were recorded using a Perkin-Elmer Spectrum One spectrophotometer. Thermogravimetric analyses (TGA) were performed in a TGA Q500−0885 equipment of TA Instrumentsal analysis. Samples were heated from 30 °C up to 800 °C at a heating rate of 10 °C/min under an air atmosphere. Scanning electron microscopy (SEM) measurements were obtained using a field emission scanning electron microscope (FE-SEM) (Hitachi, SU 8000, Japan) at 30 kV in transmitted electron imaging mode. Besides, SEM micrographs were taken using a Philips XL30 with an acceleration voltage of 25 kV. Samples were prepared from dispersions of particles which were dropped onto a carbon-coated copper grid. SEM samples were coated with gold−palladium (80/20) prior to scanning. The particle size distributions of the synthesized polymeric and hybrid particles as well as of the magnetic nanoparticles were estimated using the image analysis software ImageJ. X-ray diffraction (XRD) patterns were recorded in the reflection mode by using a Bruker D8 Advance diffractometer provided with a PSD Vantec detector. Cu Kα radiation (λ = 0.154 nm) was used, operating at 40 kV and 40 mA. The parallel beam optics was adjusted by a parabolic Göbel mirror with a horizontal grazing incidence Soller slit of 0.12° and a LiF monochromator. The equipment was calibrated with different standards. A step scanning mode was employed for the detector. The diffraction scans were collected within the range of 2θ = 4−90°, with a 2θ step of 0.024° and 0.5 s per step. The field dependence of the magnetization for the particles was obtained using a superconducting quantum interface device magnetometer (SQUID, Quantum Design, MPMS-XL) operated at 300 K. UV−vis spectra were recorded in a PerkinElmer Lambda 16 spectrophotometer. Particles were dispersed by using a Vibra-cell 75186 ultrasonic processor.

RESULTS AND DISCUSSION

Gold-Decorated Polymeric Particles (Scheme 1B). *Synthesis of the Polymeric Microparticles Containing Dopamine Groups (DMA-co-EGDMA).* Series of cross-linked microspheres containing catechol moieties were successfully synthesized via precipitation polymerization of dopamine methacrylamide (DMA) and ethylene glycol dimethacrylate (EGDMA). All the reactions were carried out under similar experimental conditions varying the proportion of DMA and EGDMA, and, accordingly, the cross-linking density and the content of the active catechol groups. The formation of stable microspheres in the precipitation polymerization is strongly dependent on the degree of cross-linking. In this sense, relatively high amount of cross-linking agent is necessary, normally over 20%, to prevent fusion between forming particles.[35] Figure 1 shows the SEM micrographs of the obtained microspheres with different content of EGDMA.

In all cases the content of the cross-linking agent used in the reaction was high enough to obtain stable spherical particles with smooth surface. As expected, the particle size decreases as the concentration of EGDMA in monomer composition increases because a large number of nuclei were formed in the initial stage of the reaction as a consequence of the lower solubility of these nuclei with high content cross-linker. In general, they present narrow distributions though when low amount of cross-linker was used, the particle size shows bimodal distribution. This may arise from the reaction mechanism in the precipitation polymerization proposed previously.[36]

The obtained particles were first characterized by FTIR to analyze their chemical composition. Figure 2 depicts the spectra of the microspheres synthesized varying the content of DMA in the feed. The intensity of absorption bands characteristic of the DMA at 3443 and 1651 cm^{-1} which are attributed to the

dx.doi.org/10.1021/ma4003566 | *Macromolecules* 2013, 46, 2951−2962

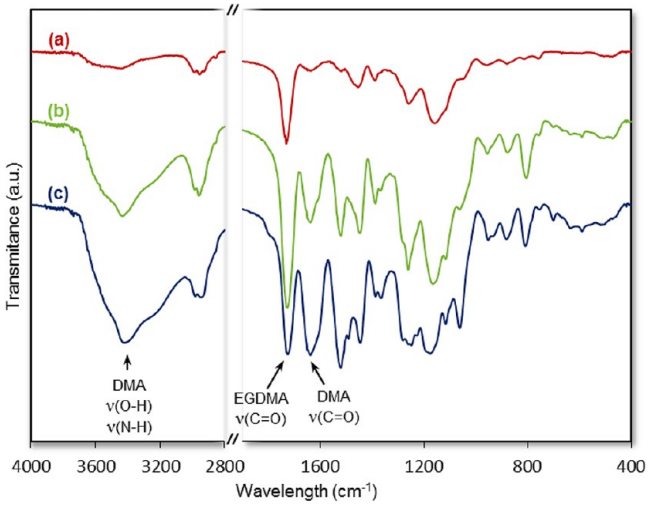

Figure 2. FTIR spectra of the synthesized DMA-*co*-EGDMA microspheres. DMA/EGDMA ratio: (a) 20/80, (b) 55/45, and (c) 80/20 wt %.

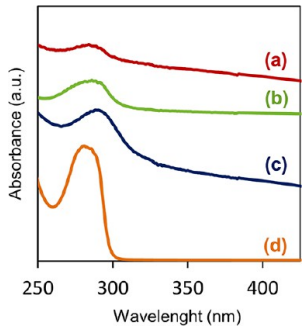

Figure 3. UV−vis spectra of the synthesized DMA-*co*-EGDMA microspheres. DMA/EGDMA ratio: (a) 20/80, (b) 55/45, and (c) 80/20 wt %. (d) DMA monomer.

phenolic hydroxyl groups and the carbonyl of the amide, respectively, increases with the increasing content of DMA in the feed composition. On the contrary, the bands at 1732 cm^{-1} associated with the ester C═O stretching in the EGDMA tends to diminish, as expected from the employed feed composition. Therefore, the content of DMA units and, consequently, of active catechol groups in the synthesized particles can be varied and controlled by the comonomer composition in the initial feed.

The appearance of two weak bands at 1482 and 1738 cm^{-1} indicates the presence of oxidative forms of catechols. Although the peak at 1738 cm^{-1} cannot be used to establish the existence of oxidative forms due to EGDMA contribution, the band centered at 1484 cm^{-1} can likely be assigned to a C−O stretching vibration of semiquinones.[37] This peak is more notable in spectra of the microspheres with higher content of DMA (Figure 2, parts b and c). Thus, indicating the presence of small percent of oxidative form.

It is well-known the easy oxidation of catechol units to their quinine form,[38] which can then participate in a variety of reactions, including the cross-linking reaction[39] and thiol-catechol reaction.[40,41] However, the quinone form is considered to be not adhesive, also losing its reductive properties.[42] As commented above, the FTIR spectra only show small bands associated with the oxidized form; therefore, we could assume that most of the catechol moieties of the synthesized microspheres are intact and can act subsequently as reducing agents for the synthesis and surface stabilization of gold nanoparticles. The UV−vis spectra of the particles also confirm this fact where it can be observed a single absorption peak at 280 nm characteristic of the catechol form and the absence of a band at about 395 nm expected for the quinone form (Figure 3).

Decoration of the DMA-co-EGDMA Microspheres with Gold Nanoparticles. Gold nanoparticles are commonly generated by redox reactions using reducing agents such as sodium borohydride or sodium citrate. As commented above, catechol containing molecules present redox activity and can also reduce metal cations, i.e., gold, into neutral metal atoms.[5,43−45] The two-electron oxidation of the catechol hydroxyl groups to form the hydroquinone derivative, concurrently reduces Au^{3+} to Au^0. Additionally, the catechol groups at the surface of the synthesized microspheres can form robust binding to metals. Hence, the reduced elemental metals could be bonded to the microspheres as seed precursors for the growth of metal nanoparticles through the atom-by-atom growth with the reduction of the metallic anions.[6,46] The oxidized quinines exhibit significantly decreased binding affinity although it is described that the catechol and quinone structures are in equilibrium state in aqueous solution.[47] As a consequence of these properties it is expected to form and anchor gold nanoparticles directly from an aqueous solution of $HAuCl_4$ on the surface of the microsphere without the addition of any exogenous reducing agent. Indeed, the solution immediately turns to deep purple as a result of the gold nanoparticles formation. Figure 4 shows the FE-SEM images of the DMA-*co*-EGDMA microspheres decorated with the gold nanoparticles. Interestingly, the size of the formed gold nanoparticles seems to be dependent on the DMA content in the microsphere, increasing the size as the amount of DMA decreases.

The average size of the gold NPs attached to the microsphere with different content on catechol groups was analyzed more extensively by XRD. The diffractograms show the typical diffraction peaks at 2θ = 38.3°, 44.5°, 64.7°, 77.7°, 81.9°, attributed to (111), (200), (220), (311), and (222) planes of gold, respectively, in a cubic phase (Figure 5).[48] Scherrer's equation[49] was used to estimate the average crystallite size using the peak broadening of the more intense peaks (111) of each diffractogram and taking into account the instrumental broadening of the diffractometer. On the basis of this equation the average size was calculated approximately as 30, 50, 58 nm for the DMA-*co*-EGDMA microspheres with a DMA/EGDMA ratio of 80/20, 55/45 and 20/80 wt %, respectively. These values are in good agreement with the microscopy measurements, confirming the decrease in size as the proportion of DMA augment in the microsphere.

Besides, this size diminishment is accompanied by an increase in the total content of gold anchored to the polymeric particles with higher content of catechol groups. The total amount of gold on the particle surface was quantitative measured by TGA resulting in 18, 11, and 8 wt % for DMA/EGDMA ratio of 80/20, 55/45 and 20/80 wt %, respectively (Figure 6). Therefore, we can conclude that the amount of catechol residues within the microspheres is crucial for the formation, stabilization and growth of the gold nanoparticles. Higher amount of catechol groups generates larger content of small-sized Au nanoclusters.

dx.doi.org/10.1021/ma4003566 | *Macromolecules* 2013, 46, 2951−2962

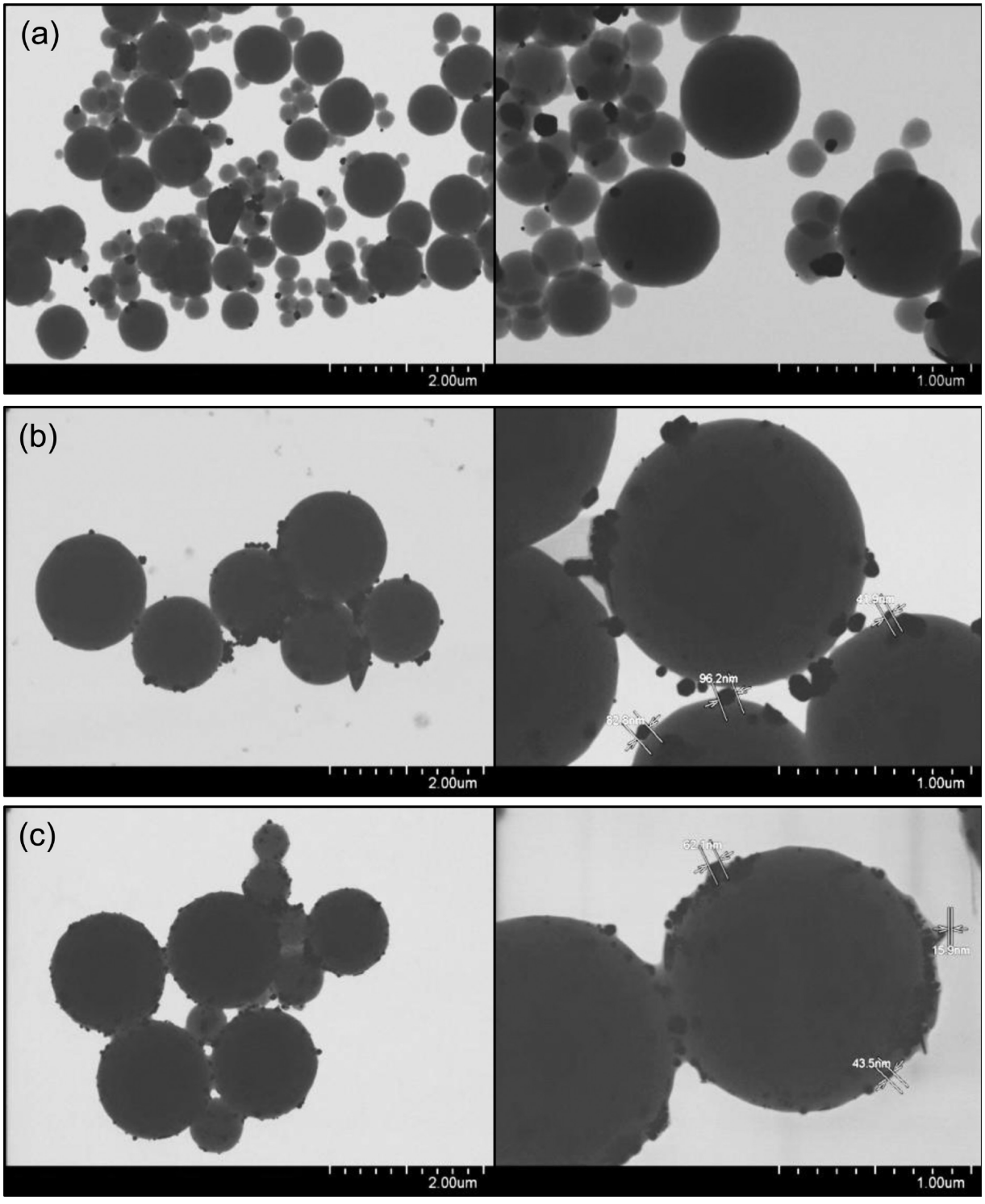

Figure 4. FE-SEM images of the DMA-*co*-EGDMA@Au hybrid microspheres. DMA/EGDMA ratio: (a) 20/80, (b) 55/45, and (c) 80/20 wt %.

Moreover, in order to corroborate that residual weight is only due to the gold present in the samples, TGA of polymeric particles before anchored the metal nanoparticles was made. The inset shows the thermogram of the particles with 80/20 DMA/EGDMA composition. The total loss of weight indicates complete decomposition of the polymer.

The catalytic activity of the synthesized hybrid microspheres was investigated by choosing as a model reaction the reduction of 4-nitrophenol to 4-aminophenol in the presence of $NaBH_4$. Visually, as the reaction proceeds, the solution color changes gradually from yellow to colorless. The reactions were monitored by UV−vis spectroscopy as illustrated in Figure 7. The absorption peak at 400 nm, characteristic of 4-nitrophenolate ions, gradually decreases in intensity. Meanwhile, a new peak at 300 nm, the typical absorption of 4-AP, appears and increases in intensity. As can be seen in Figure 7, when synthesized DMA-*co*-EGDMA@Au hybrid microspheres were used, the reaction was completed in less than 90 min with only a total weight of catalyst of 0.05 mg exhibiting relatively good catalytic performance comparable with standard systems[50,51]

dx.doi.org/10.1021/ma4003566 | *Macromolecules* 2013, 46, 2951−2962

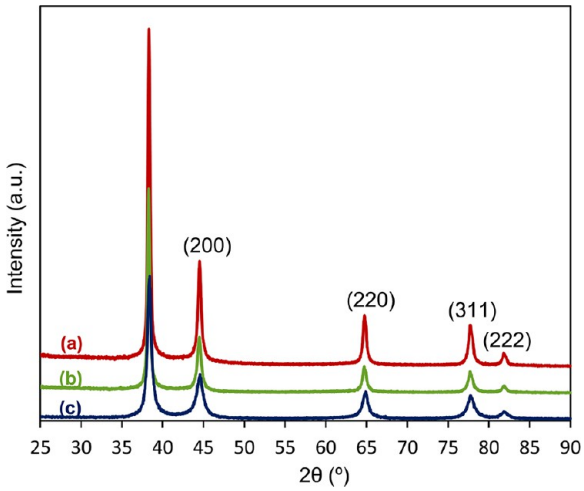

Figure 5. DRX diffractograms of DMA-*co*-EGDMA@Au hybrid microspheres. DMA/EGDMA ratio: (a) 20/80, (b) 55/45, (c) 80/20 wt %.

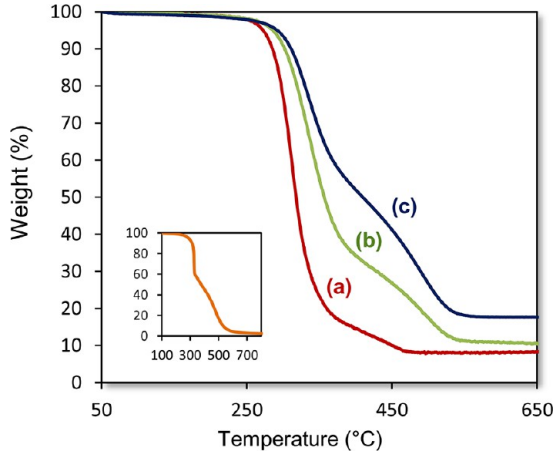

Figure 6. TGA thermograms of DMA-*co*-EGDMA@Au hybrid microspheres. DMA/EGDMA ratio: (a) 20/80, (b) 55/45, and (c) 80/20. Inset: TGA of DMA-*co*-EGDMA particles with DMA/EGDMA ratio of 80/20.

and supported systems[29,45] previously reported. As expected the reduction process is much faster when the catalytic particles contain higher gold content and smaller particle sizes thus larger surface area.

In summary, microspheres with high loading of tiny gold nanoparticles were synthesized through a facile and novel method based on the catechol chemistry in which the content of DMA within the microsphere can be easily varied and, consequently, the amount and the size of the gold NPs anchored to the surface accordingly controlled.

Magnetite-Encapsulated and Gold Nanoparticles-Decorated Microparticles (Scheme 1C). *Preparation of Magnetite/DMA-co-EGDMA Particles (Fe_3O_4@DMA-co-EGDMA).* Although the synthesized microspheres demonstrated to be an adequate support for the in situ growth of gold NPs with high catalytic capability, their recovery and reusability is rather difficult. As an alternative we next consider the incorporation of magnetic nanoparticles in cross-linked polymeric particles that would make the particles more suitable for catalysis purpose, easily to isolate from the media by an external magnet and reuse in the next cycle. Herein, the magnetic hybrid particles were prepared via seeded precipitation polymerization consisting in the radical copolymerization of DMA and EGDMA in the presence of modified magnetite nanoparticles (Fe_3O_4@DMA NPs) as seeds. Magnetite nanoparticles were first prepared by thermal decomposition process followed by their modification with the bioinspired dopamine methacrylamide monomer to incorporate vinyl groups at the particle surface following an approach previously described for our group (Scheme 1).[34,52] Figure 8a shows the FE-SEM images of the synthesized magnetite nanoparticles with an average edge length of 14 ± 2 nm.

The precipitation polymerization reaction of DMA and EGDMA in the presence of Fe_3O_4@DMA NPs was carried out according to previously reported procedure[52] with few modifications. On the basis of the results described above, a monomer feed composition consisting of 45 wt % of DMA and 55 wt % of EGDMA was used to ensure the synthesis of highly cross-linked particles with certain integrity, high content of DMA and moderate particle size distribution. FE-SEM measurements reveal the formation of continuous polymeric layers that completely cover the magnetic seeds, resulting in core−shell structures (Figure 8b) with a shell thickness of about 190 nm. Although the obtained particles appear in aggregated structures, in the SEM image (Figure 8c) most of the particles remain individual having a mean diameter of around 1.0 ± 0.2 μm. Then the content of Fe_3O_4@DMA NPs incorporated into the polymeric particles containing catechol residues was quantified by thermogravimetric analysis under air atmosphere, revealing a ∼20 wt % of magnetic material.

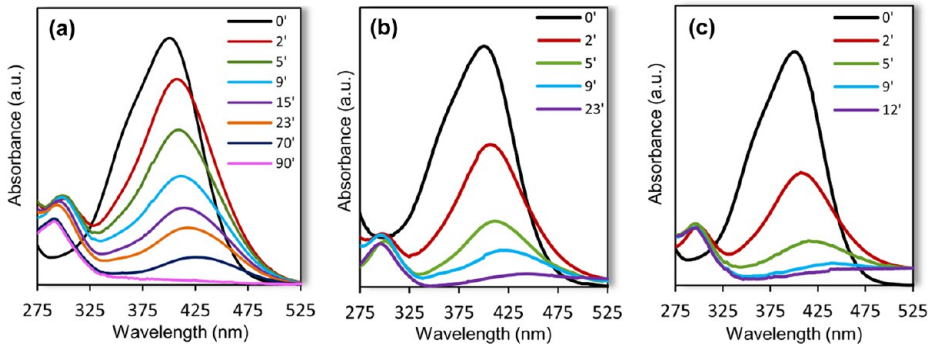

Figure 7. UV−vis spectra of the reduction of 4-nitrophenol to 4-aminophenol with $NaBH_4$ in the presence DMA-*co*-EGDMA@Au microspheres as catalysts containing a DMA/EGDMA ratio: (a) 20/80, (b) 55/45, and (c) 80/20 wt %.

dx.doi.org/10.1021/ma4003566 | *Macromolecules* 2013, 46, 2951−2962

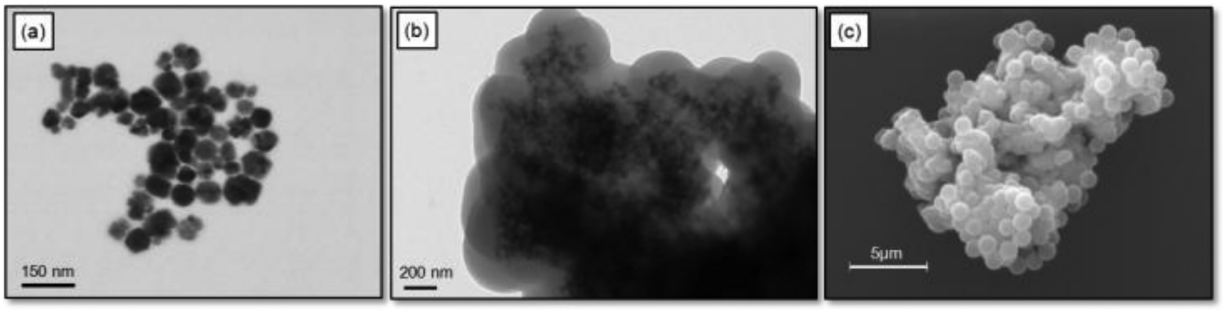

Figure 8. (a) FE-SEM images of Fe_3O_4@DMA NPs used as seed and (b and c) FE-SEM and SEM, respectively of Fe_3O_4@DMA-*co*-EGDMA hybrid magnetic particles with DMA/EGDMA ratio: 55/45 wt %.

Concerning the magnetic properties of the obtained Fe_3O_4@DMA-*co*-EGDMA hybrid magnetic particles, it was observed previously that this type of compartmentalization of magnetite nanoparticles may affect the magnetic properties. The magnetization experiments of the Fe_3O_4@DMA NPs used as seed are displayed in Figure 9, indicating high saturation magnetization

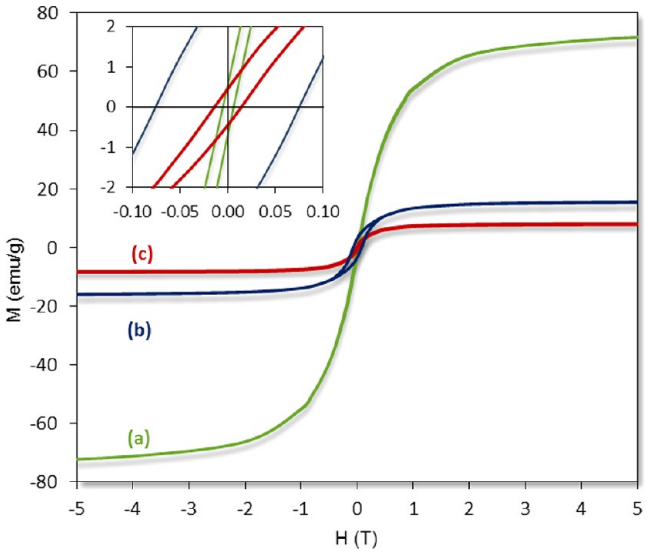

Figure 9. Magnetization curves of (a) Fe_3O_4@DMA NPs, (b) Fe_3O_4@DMA-*co*-EGDMA, and (c) DMA-*co*-EGDMA@ Fe_3O_4 hybrid microspheres.

(M_s) values (76 emu/g) and almost no hysteresis loops in the magnetization curves with negligible coercivity (~6 mT) and remanent magnetization (0.6 emu/g). As expected for their size (~14 nm) the NPs exhibit superparamagnetism.[53] However, after the formation of continuous polymeric layers covering the magnetic seeds their magnetic properties radically change. In addition to the typical decrease in saturation magnetization as a consequence of the polymeric shell, in this case to 16 emu/g, the M−H curve shows a large hysteresis loop with coercivity and remanence values of 76 mT and 3.2 emu/g, respectively. These findings reflect that the magnetite nanoparticles lost their superparamagnetic properties after their incorporation inside the polymer particle where they are touching each other in a cluster form.[52,54−56] Nevertheless, the synthesized hybrid particles exhibit sufficient magnetization for magnetic separation from a mixture solution and can be used as a magnetically recoverable catalyst support.

Subsequently, the hybrid magnetic particles which contain dopamine residues at the surface were decorated with gold nanoparticles following similar procedure used for the previous polymeric DMA-*co*-EGDMA microspheres, i.e., in situ reduction and immobilization of gold NPs by the DMA units at ambient temperature and without the addition of any other reducing agents. As shown in the FE-SEM image of Figure 10a, tiny gold NPs can be distinguished at the surface of the particles by the deepest contrast compared to the gray core associated with the magnetic NPs.

In the TGA analysis of Fe_3O_4@DMA-*co*-EGDMA@Au obtained particles, the mass fraction remaining at the end of the measurement corresponds to both magnetite and gold content of the hybrid particles. By assuming ca. 20 wt % of magnetic material as calculated previously, the analysis gives a

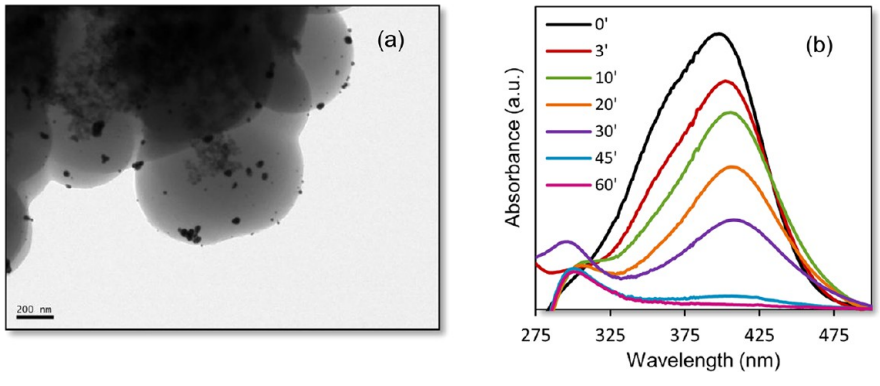

Figure 10. (a) FE-SEM image of Fe_3O_4@DMA-*co*-EGDMA@Au microspheres and (b) UV−vis spectra monitored during reduction of 4-nitrophenol to 4-aminophenol using 0.05 mg of Fe_3O_4@DMA-*co*-EGDMA@Au particles as catalyst.

dx.doi.org/10.1021/ma4003566 | *Macromolecules* 2013, 46, 2951−2962

measured value of ∼5 wt % of gold nanoparticles. This low content of Au compared to the value obtained in the case of the nonmagnetic microspheres (DMA-*co*-EGDMA@Au) may be caused by the high agglomeration of the magnetic hybrid particles which significantly reduces the surface area and provides less accessible sites to support the formation of much gold NPs. Nevertheless, the size of the gold nanoparticles is smaller than the values found for the DMA-*co*-EGDMA@Au microspheres with DMA/EGDMA of 55/45 wt %, that is ∼15 nm as calculated by DRX (Figure 11).

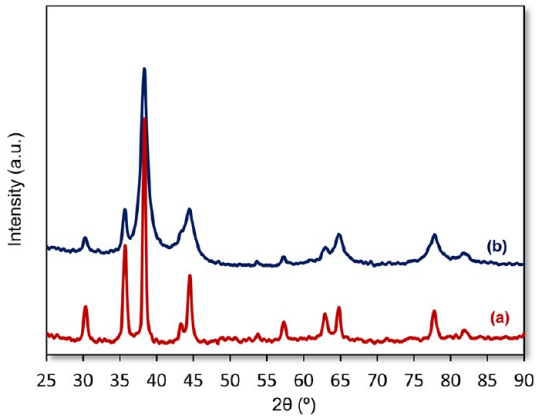

Figure 11. XRD of (a) Fe_3O_4@DMA-*co*-EGDMA@Au and (b) DMA-*co*-EGDMA@Fe_3O_4@Au hybrid microspheres.

Then, the catalytic activity of the Fe_3O_4@DMA-*co*-EGDMA@Au was evaluated through the reduction of 4-nitrophenol in the presence of $NaBH_4$. Figure 10b displays the UV−vis absorption spectra measured at different times during the progress of the reaction. It can be seen that this catalyst exhibited reasonable kinetic rate for nitrophenol reduction but lower reaction rate compared to the DMA-*co*-EGDMA@Au as a consequence of the lower content of gold nanoparticles for the same amount of total catalyst. Although the catalytic kinetic is a bit slower in the case of the magnetic Fe_3O_4@DMA-*co*-EGDMA@Au particles they demonstrate recycling properties which is a very important concern for the applicability of this material in catalysis. This catalyst can be successfully reused in at least 10 repeated processes via separation with a magnet and redispersed for the next cycle. In addition, the reaction rate does not decrease after the reuse of catalyst, indicating its excellent recyclability.

Polymeric Particles Decorated with Magnetite and Gold NPs (Scheme 1D). *Surface Decoration of the DMA-co-EGDMA Microspheres with Magnetite Nanoparticles (DMA-co-EGDMA@Fe_3O_4).* The results exposed above demonstrate the suitable potential of the synthesized hybrid Fe_3O_4@DMA-*co*-EGDMA@Au particles as recyclable catalyst system. However, they still present some drawbacks. In the hybrid particles prepared by this method, seeded precipitation polymerization, the magnetite NPs are aggregated in clustered form constituting the core of the particle. In this way the magnetic core exhibits ferrimagnetic response under a magnetic field in contrast to the superparamagnetic behavior of the individual Fe_3O_4@DMA NPs. In order to avoid the possible irreversible agglomeration associated with the ferrimagnetic properties of the magnetic particles, an alternative synthetic approach was subsequently used to prepare magnetic supports for gold NPs. This method consists on the surface attachment of magnetite nanoparticles to the DMA-*co*-EGDMA microspheres previously synthesized, giving place to raspberry-like magnetic nanocomposite microspheres (Scheme 1D) and avoiding in somehow the agglomeration of the magnetic NPs. The catechol residues of the prepared microspheres, in addition to the metal-binding ability and the reducing activity, also support a variety of reactions with organic compounds. Under oxidizing (e.g., basic) conditions, catechol/quinone reacts with thiols and amines via Michael addition (amine- and thiol-containing molecules) or Schiff base reactions (amine-containing molecules).[38]

In this study, we make use of this catechol chemistry to immobilize magnetite NPs on the surface of the DMA-*co*-EGDMA microspheres, that is, the magnetite nanoparticles were first functionalized with amine groups, Fe_3O_4@D NPs and then covalently bonded via conjugation between the amine groups and the *o*-quinone moieties of the microsphere surfaces (see Scheme 1D). Concerning the catechol/quinone groups of the polymeric microspheres, an important aspect to take into account is the degree of the catechol oxidation (content of quinone groups). A certain amount of quinone forms are necessary to introduce the magnetite NPs but at the same time, nonoxidized catechol groups are needed for the posterior in situ reduction and immobilization of gold NPs. As demonstrated by FTIR (Figure 2) a small percentage of DMA units were

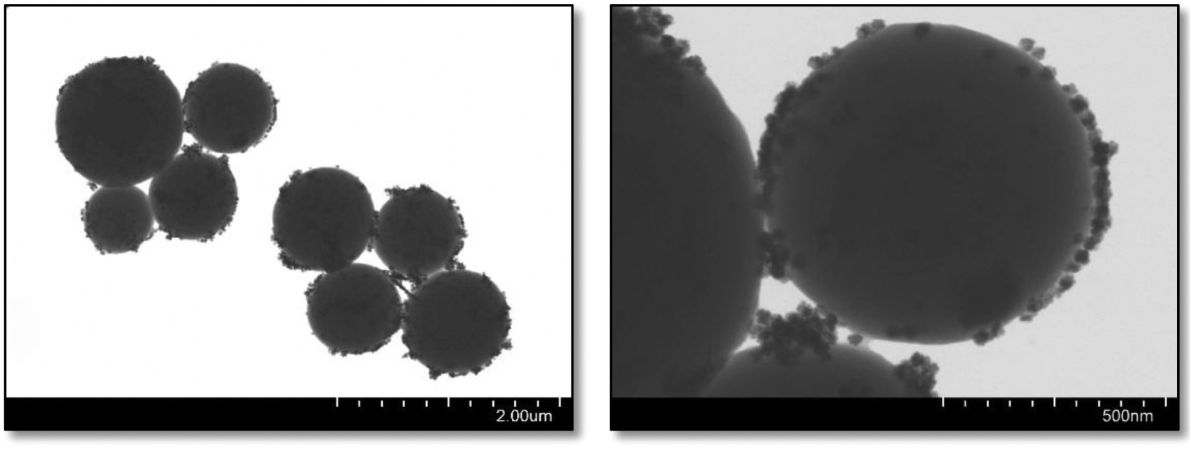

Figure 12. FE-SEM images of DMA-*co*-EGDMA@Fe_3O_4 hybrid magnetic particles with DMA/EGDMA ratio: 55/45 wt %.

dx.doi.org/10.1021/ma4003566 | *Macromolecules* 2013, 46, 2951−2962

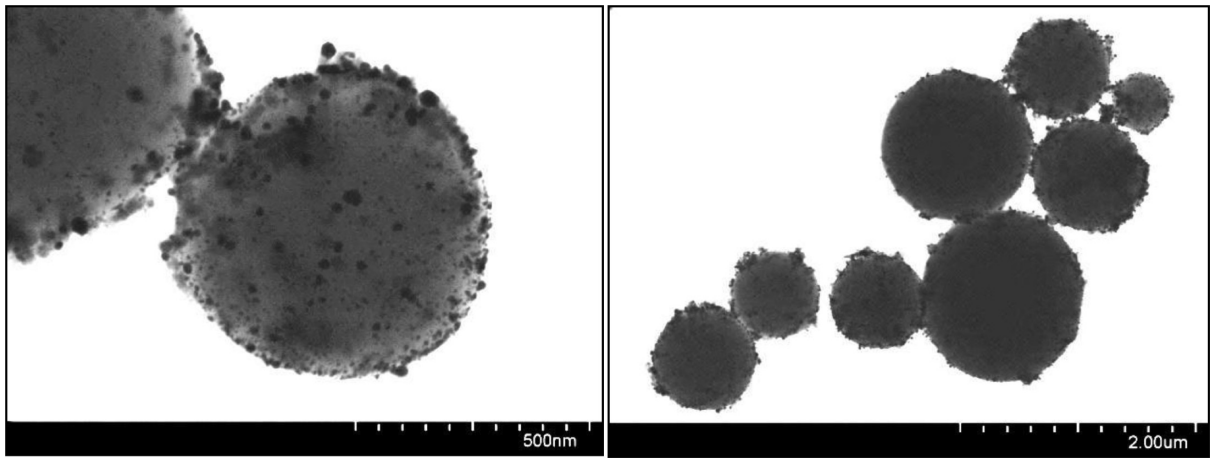

Figure 13. FE-SEM images of DMA-*co*-EGDMA@Fe_3O_4@Au hybrid magnetic particles with DMA/EGDMA ratio: 55/45 wt %.

oxidized after the preparation of the polymeric microspheres. These quinone groups were utilized for the incorporation of the magnetite NPs functionalized with amine groups avoiding in this case any previous oxidative step. Since the magnetic nanocomposite microspheres will be subsequently utilized as support for the growth and stabilization of gold NPs the reaction was carried out in DMF instead of oxidative basic solution. In this way there would be available catechol groups at the surface for gold NPs. From the FE-SEM images (Figure 12), it can be seen that plenty of magnetite nanoparticles are well dispersed and distributed onto the particle surface. The TGA analysis indicates Fe_3O_4 content of approximately 7 wt %.

In contrast to the previously described particles with a magnetic core, the magnetization curve in Figure 10 illustrates negligible magnetic remanence (0.45 emu/g) and the absence of coercive force (15 mT), which indicates the superparamagnetic nature of the DMA-*co*-EGDMA@ Fe_3O_4 particles. However, saturation magnetization decreases significantly up to 8 emu/g. This is a consequence of the large percentage of polymer ca. 93 wt %.

Forming and Anchoring of Gold Nanoparticles onto the Surface of the DMA-co-EGDMA@Fe_3O_4 particles (DMA-co-EGDMA@Fe_3O_4@Au). Finally, DMA-*co*-EGDMA@Fe_3O_4 microparticles were mixed $HAuCl_4$ solution for the in situ decoration of Au NPs on the surface. Here, the nonoxidazed catechol groups of the DMA units serve as reducing agent for the synthesis of gold NPs. FE-SEM measurements (Figure 13) show that relatively large amounts of Au NPs (9 wt % gold content) with tiny size (13 nm in diameter calculated by RDX, Figure 11) are homogeneously attached onto the surface.

The catalytic performance of these DMA-*co*-EGDMA@ Fe_3O_4@Au microspheres were then investigated and compared with the other obtained catalytic systems prepared herein. When 0.05 mg of catalyst is used, as in the rest of the systems, the reduction of the 4-aminophenol was completed in 60 min (Figure 14).

The reaction rate is almost similar when compared with that by the Fe_3O_4@DMA-*co*-EGDMA@Au and slower than the nonmagnetic microspheres of DMA-*co*-EGDMA@Au. Therefore, it seems that the total content of gold NPs is crucial and the main parameter that influences the catalytic process. In relation to the recycling possibilities of this last synthesized, the results demonstrate magnetic separation ability and reusability which can be repeatedly applied for nearly complete reduction of nitrophenols for six successive cycles. However, the activity

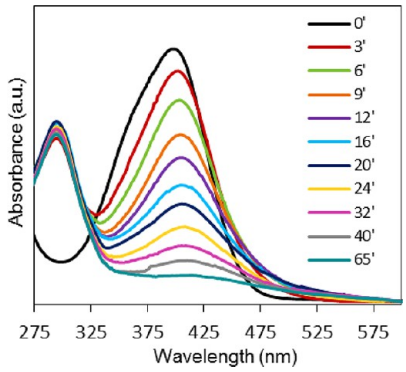

Figure 14. UV−vis spectra during the catalytic reduction of 4-NP by the DMA-*co*-EGDMA@Fe_3O_4@Au hybrid particles.

decreases after the catalyst recycling from 1 to 3 h of reaction time. Such diminishment of activity may be probably attributed to the loss of catalyst after periodic cycles because the magnetization value of these particles is rather low (see Figure 9). As a result their separation from the solution by a magnet would be relatively slow. Another explanation of this decrease in activity could be the binding of the generated aminophenols to the surface of the Au NPs resulting in the blockade of reactive sites.[57] The catalytic reaction was then carried out successive times in the same cuvette without separation of the catalyst and adding the nitrophenols repeatedly. In this condition the catalytic capability was maintained over many successive reaction runs. Consequently, the blocking of the Au NPs by absorbed nitrophenol molecules was finally discarded.

■ CONCLUSIONS

Different catalytic systems with excellent activity were synthesized by a facile and versatile approach consisting on the preparation of cross-linked particles containing dopamine residues. This approach allows us to tune the degree of active catechol moieties available at the surface by controlling the initial feed composition. These functional polymeric particles with numerous anchoring sites serve as supports for the incorporation via catecholic chemistry of magnetite and gold nanoparticles providing the recyclability and the catalytic activity, respectively. This synthetic strategy provides the advantage of a facile preparation under mild reaction conditions, without heat treatments, organic solvent or

dx.doi.org/10.1021/ma4003566 | *Macromolecules* 2013, 46, 2951−2962

additional reducing agents, during the whole process of functionalization. The content and the size of the attached gold nanoparticles seem to be dependent on the catechol content in the polymeric microspheres, higher amount of smaller gold NPs are anchored with increasing DMA content. Similarly, the catalytic activity of the prepared systems varies according the gold nanoparticles content. The reduction process is much faster when the catalytic particles contain higher gold content and smaller particle sizes, thus, larger surface area. Furthermore, the hybrid systems containing also magnetite nanoparticles exhibit good magnetic capability for recovery and reusability as demonstrated over successive reaction cycles. This strategy is, therefore, postulated as an attractive alternative to prepare a huge variety of promising materials.

AUTHOR INFORMATION

Corresponding Author

*E-mail: (A.M.-B.) sbonilla@ictp.csic.es; (M.F.-G.) martafg@ictp.csic.es.

Notes

The authors declare no competing financial interest.

ACKNOWLEDGMENTS

This work was financially supported by the MINECO (Project MAT2010-17016). M. Álvarez-Paino, A. Muñoz-Bonilla and G. Marcelo acknowledge MINECO and CSIC financial support for their FPI grant, Juan de la Cierva and JAEdoc contracts.

REFERENCES

(1) Lee, Y.; Lee, H.; Kim, Y. B.; Kim, J.; Hyeon, T.; Park, H.; Messersmith, P. B.; Park, T. G. *Adv. Mater.* **2008**, *20*, 4154−4157.

(2) Cheng, K.; Peng, S.; Xu, C.; Sun, S. *J. Am. Chem. Soc.* **2009**, *131*, 10637−10644.

(3) Nam, H. J.; Kim, B.; Ko, M. J.; Jin, M.; Kim, J. M.; Jung, D.−Y. *Chem.—Eur. J.* **2012**, *18*, 14000−14007.

(4) Ye, Q.; Zhou, F.; Liu, W. *Chem. Soc. Rev.* **2011**, *40*, 4244−4258.

(5) Black, K. C. L.; Liu, Z.; Messersmith, P. B. *Chem. Mater.* **2011**, *23*, 1130−1135.

(6) Xu, H.; Shi, X.; Ma, H.; Lv, Y.; Zhang, L.; Mao, Z. *Appl. Surf. Sci.* **2011**, *257*, 6799−6803.

(7) Marcelo, G.; Munoz-Bonilla, A.; Fernandez-García, M. *J. Phys. Chem. C* **2012**, *116*, 24717−24725.

(8) Gnichwitz, J. F.; Marczak, R.; Werner, F.; Lang, N.; Jux, N.; Guldi, D. M.; Peukert, W.; Hirsch, A. *J. Am. Chem. Soc.* **2010**, *132*, 17910−17920.

(9) Xie, J.; Xu, C. J.; Xu, Z. C.; Hou, Y. L.; Young, K. L.; Wang, S. X.; Pourmond, N.; Sun, S. H. *Chem. Mater.* **2006**, *18*, 5401−5403.

(10) Na, H. B.; Pauli, G.; Rosenberg, J. T.; Ji, X.; Grant, S. C.; Mattoussi, H. *ACS Nano* **2012**, *6*, 389−399.

(11) Saville, S. L.; Stone, R. C.; Qi, B.; Mefford, O. T. *J. Mater. Chem.* **2012**, *22*, 24909−24917.

(12) Lu, A. -H.; Salabas, E. L.; Schüth, F. *Angew. Chem., Int. Ed.* **2007**, *46*, 1222−1244.

(13) Laurent, S.; Forge, D.; Port, M.; Roch, A.; Robic, C.; Elst, L. V.; Muller, R. N. *Chem. Soc. Rev.* **2008**, *108*, 2064−2110.

(14) Thomas, L. A.; Dekker, L.; Kallumadil, M.; Southern, P.; Wilson, M.; Nair, S. P.; Pankhurst, Q. A.; Parkin, I. P. *J. Mater. Chem.* **2009**, *19*, 6529−6535.

(15) Kumar, C. S. S. R.; Mohammad, F. *Adv. Drug Delivery Rev.* **2011**, *63*, 789−808.

(16) Bao, J.; Chen, W.; Liu, T.; Zhu, Y.; Jin, P.; Wang, L.; Liu, J.; Wei, Y.; Li, Y. *ACS Nano* **2007**, *1*, 293−298.

(17) Hu, J.; Qian, Y.; Wang, X.; Liu, T.; Liu, S. *Langmuir* **2012**, *28*, 2073−2082.

(18) Shylesh, S.; Thiel, W. R.; Schünemann, V. *Angew. Chem., Int. Ed.* **2010**, *49*, 3428−3459.

(19) Hu, A.; Liu, S.; Lin, W. *RSC Adv.* **2012**, *2*, 2576−2580.

(20) Hu, A.; Yee, G. T.; Lin, W. *J. Am. Chem. Soc.* **2005**, *127*, 12486−12487.

(21) Marcelo, G.; Munoz-Bonilla, A.; Fernandez-García, M. *J. Phys. Chem. C* **2012**, *116*, 24717−24725.

(22) Ge, J.; Huynh, T.; Hu, Y.; Yin, Y. *Nano Lett.* **2008**, *8*, 931−934.

(23) Corma, A.; García, H. *Chem. Soc. Rev.* **2008**, *37*, 2096−2126.

(24) Hashmi, A. S. K.; Hutchings, G. J. *Angew. Chem., Int. Ed.* **2006**, *45*, 7896−7936.

(25) Choudhary, T. V.; Goodman, D. W. *Top. Catal.* **2002**, *21*, 25−34.

(26) Choudhary, T. V.; Goodman, D. W. *Appl. Catal., A* **2005**, *32*, 32−36.

(27) Stratakis, M.; García, H. *Chem. Rev.* **2012**, *112*, 4469−4506.

(28) Zheng, N.; Stucky, G. D. *J. Am. Chem. Soc.* **2006**, *128*, 14278−14280.

(29) Liu, B.; Zhang, W.; Feng, H.; Yang, X. *Chem. Commun.* **2011**, *47*, 11727−11729.

(30) Ham, H. O.; Liu, Z.; Lau, K. H. A.; Lee, H.; Messersmith, P. B. *Angew. Chem., Int. Ed.* **2011**, *50*, 732−736.

(31) Lee, H.; Lee, B. P.; Messersmith, P. B. *Nature* **2007**, *448*, 338−342.

(32) Guardia, P.; Labarta, A.; Batlle, X. *J. Phys. Chem. C* **2010**, *115*, 390−396.

(33) Marcelo, G.; Munoz-Bonilla, A.; Rodríguez-Hernández, J.; Fernández-García, M. *Polym. Chem.* **2013**, *4*, 558−567.

(34) Muñoz-Bonilla, A.; Marcelo, G.; Casado, C.; Teran, F. J.; Fernández-García, M. *J. Polym. Sci., Part A: Polym. Chem.* **2012**, *50*, 5087−5096.

(35) Ha, M.; Lee, K.; Choe, S. *Polymer* **2008**, *49*, 4592−4601.

(36) Shim, S. E.; Yang, S.; Soonja, C. *J. Polym. Sci., Part A: Polym. Chem.* **2004**, *42*, 3967−3974.

(37) Amstad, E.; Gehring, A. U.; Fischer, H.; Nagaiyanallur, V. V.; Hähner, G.; Textor, M.; Reimhult, E. *J. Phys. Chem. C* **2011**, *115*, 683−691.

(38) Lee, H.; Dellatore, S. M.; Miller, W. M.; Messersmith, P. B. *Science* **2007**, *318*, 426−430.

(39) Guvendiren, M.; Messersmith, P. B.; Shull, K. R. *Biomacromolecules* **2008**, *9*, 122−128.

(40) Lee, Y.; Chung, H. J.; Yeo, S.; Ahn, C.-H.; Lee, H.; Messersmith, P. B.; Park, T. G. *Soft Matter* **2010**, *6*, 977−983.

(41) Cui, J.; Yan, Y.; Such, G. K.; Liang, K.; Ochs, C. J.; Postma, A.; Caruso, F. *Biomacromolecules* **2012**, *13*, 2225−2228.

(42) Faure, E.; Falentin-Daudre, C.; Jerome, C.; Lyskawa, J.; Fournier, D.; Woisel, P.; Detrembleur, C. *Prog. Polym. Sci.* **2013**, *38*, 236−270.

(43) Ho, J. A.; Chang, H. C.; Su, W. T. *Anal. Chem.* **2012**, *84*, 3246−3253.

(44) Lee, Y.; Park, T. G. *Langmuir* **2011**, *27*, 2965−2971.

(45) Qu, W.-G.; Wang, S.-M.; Hu, Z.-J.; Cheang, T.-Y.; Xing, Z.-H.; Zhang, X.-J.; Xu, A.-W. *J. Phys. Chem. C* **2010**, *114*, 13010−13016.

(46) Hamamoto, K.; Kawakita, H.; Ohto, K.; Inoue, K. *React. Funct. Polym.* **2009**, *69*, 694−697.

(47) Lee, H.; Rho, J.; Messersmith, P. B. *Adv. Mater.* **2009**, *21*, 431−434.

(48) JCPDS-International Center for Diffraction Data, PCPDFWIN v. 1.30, 04−0784.

(49) Guinier, A. *X-Ray Diffraction in Crystals, Imperfect Crystals, and Amorphous Bodies*; Dover: Mineola, NY, 1994; Chapter 5.

(50) Pradhan, N. *Colloids Surf., A* **2002**, *196*, 247−257.

(51) Fenger, R.; Fertitta, E.; Kirmse, H.; Thunemann, A. F.; Rademann, K. *Phys. Chem. Chem. Phys.* **2012**, *14*, 9343−9349.

(52) Álvarez-Paino, M.; Marcelo, G.; Muñoz-Bonilla, A.; Rodríguez-Hernández, J.; Fernández-García, M. *Polym. Chem.* **2013**, *4*, 986−995.

(53) Wagner, C. D.; Davis, L. E.; Zeller, M. V.; Taylor, J. A.; Raymond, R. H.; Gale, L. H. *Surf. Interface Anal.* **1981**, *3*, 211−225.

(54) Vollath, D. *Adv. Mater.* **2010**, *22*, 4410−4415.

(55) Lin, X.-M.; Samia, A. C. S. *J. Magn. Magn. Mater.* **2006**, *305*, 100−109.
(56) You, X.; He, R.; Gao, F.; Shao, Pan, J. B.; Cui, D. *Nanotechnology* **2007**, *18*, 035701.
(57) Lin, F. −H.; Doong, R.-A. *J. Phys. Chem. C* **2011**, *115*, 6591−6598.